1

2

3

4

5

6

7

8 **Mechanism of microfibril contraction and anisotropic dimensional changes**

9 **for cells in wood treated with aqueous NaOH solution**

10

11

12

13 **Takato Nakano***

14

15

16

17

18

19

20

21

26 * Laboratory of Biomaterials Design, Division of Forest and Biomaterials Science, Graduate

27 School of Agriculture, Kyoto University, Kita-Shirakawa, Kyoto, 606-8502 Japan.

28 **Abstract**

29   Anisotropic swelling of wood samples was observed upon treatment with an aqueous

30 NaOH solution with 0 to 0.20 fraction concentrations. At NaOH concentrations less than 0.10,

31 the swelling occurred only along the tangential axis (T) and not along the radial (R) or

32 longitudinal (L) axes. At greater NaOH levels, the swelling was even more pronounced along T

33 with shrinkage along the other axes. These anisotropic changes along R and L were closely

34 related to the crystallinity of microfibrils in the wood cell wall and simulated with a cell structure

35 model. This exercise revealed microfibril contraction and matrix swelling in the wood cell wall

36 upon NaOH treatment. The observed anisotropy in cross section was caused by differences in

37 the microfibril angles (LR and LT) with the cell wall.

38

39

40

Introduction

Wood samples treated with aqueous NaOH show characteristic dimensional change, especially interesting along the longitudinal axis. Stöchmann (1971a, 1971b) discussed this phenomenon in detail and thermodynamically characterized the contraction of microfibrils in the wood cell wall, though the contraction mechanism of microfibrils themselves was not clarified. This contraction along the longitudinal axis is also induced by other alkaline solutions, the degree of which increases as NaOH < KOH < LiOH at the same concentration (Nakano, 1988a, 1988b, 1989). Nakano *et al.* (2000) found from relaxation behavior and temperature dependence studies that this contraction was due to the entropy elastic force of cell wall microfibrils, and formulated a relationship between the sample length, the microfibril dimensions, and microfibril angle.

Treatment with aqueous alkaline solutions also yields changes along the radial and tangential axes, which are negative and positive, respectively (Stöckmann, 1971a, 1971b), while the sum of their changes remains nearly constant (Ishikura and Nakano, 2007). The mechanism and a quantitative relationship between these anisotropic changes have not yet been elucidated. In the present work, the relationship between changes along all three axes upon exposure of wood samples to aqueous NaOH was established from simulations of a cell wall model. The results reported herein provide information about not only the anisotropic swelling of wood but also about the structure of the wood cell wall.

Material and Methods

The validity of the cell wall model employed herein was examined by comparing experimental data reported by Ishikura and Nakano (2007) with data calculated in the present work. Preparation condition in their report is followed. Yezo spruce, Saghalin fir, and Japanese larch, all soft woods that exhibit small microfibril angles, were prepared. Samples with dimensions of $20(R) \times 20(T) \times 0.5(L)$ mm, where R, T, and L correspond to the radial, tangential, and longitudinal axes, were soaked in aqueous NaOH solution with 0 to 0.20 fraction concentrations after drying under vacuum at room temperature over P_2O_5 for four days. The

71 samples were stored at room temperature for two days and then washed in distilled water for one

72 week.   Changes along each axis were calculated from the observed differences between wet

73 dimensions after NaOH treatment and the same measurements after soaking in distilled water

74 without NaOH treatment. Their dimensions were measured by a slide calipers for R and T and a

75 micrometer for L.

76   The crystallinity of the wood samples were determined from X-ray diffraction data

77 obtained on the LR-plane at 30 kV, 100 mA, and 2 °/min.   The degree of crystallinity was

78 calculated from an the diffraction profile in the scanning range $10 - 32°$. The profile was isolated

79 to two parts of a non-crystalline and a crystalline, after subtracting air-scattering.   The degree

80 of crystallinity was defined as fraction of the crystalline reflection area to the gross area.   As for

81 the same samples, microfibril angles were freshly in this work measured by X-ray irradiation to

82 know the effect of NaOH treatment on microfibril angles. In order to have higher precision

83 LR-plane of a sample was measured at 40kV and 30 mA, and then were calculated according to

84 Cave's method.

85

86 **Results and discussion**

87

88 **Characterization of the dimensional change**

89

90   Figure 1 represents experimental results, in which NaOH treatment induces

91 dimensional changes not only along the longitudinal axis but also along the radial and tangential

92 axes with $\Delta R / R < \Delta T / T$ in the cross section.   At NaOH concentrations, [NaOH], greater than

93 0.10 fraction concentration, $\Delta R/R$ and $\Delta T / T$ values were less than and greater than zero,

94 respectively.   It is clearly found that this anisotropically dimensional change differs from that

95 induced under water adsorption.

96   A suitable cell model is necessary to discuss the characteristic dimensional changes

97 shown in Fig. 1. Various cell models have been proposed to study features such as the anisotropic

98 swelling and shrinkage of wood and wood cells, including models proposed by Barber and Meylan

99 (1967), Yamamoto (1999), and Neagu and Gamstedt (2007), and the simplified model by Fratzl

100 (2008). Salmèn and Burgert (2009) reviewed recent reports describing cell -wall models. The

101 modern cell model considers anisotropic microfibrils embedded in an elastic isotropic matrix; the

102 constitutive equation is derived under the equilibrium condition with adsorbed water in which

103 the matrix is isotropically swelling and microfibrils restrict this swelling. The microfiber angle is

104 an important factor for anisotropic dimensional change in the longitudinal direction and

105 perpendicular to the longitudinal direction. That is, the model is cylindrical. On the other hand,

106 Preston (1942) and Sadoh and Kingston (1967) examined anisotropic swelling considering the

107 geometrical deformation due to a swelling factor and some restraint.

108 Analysis of dimensional change should consider the interaction between microfibrils and

109 the matrix for the anisotropy of a cross-section. A model of equilibrium between the matrix and

110 microfibril restriction appears not to be suitable for simulation of anisotropic dimensional change

111 because there is insufficient information on microfibril movement.

112 We follow the approach of Sadoh and Kingston (1967) in the discussion below.

113 Dimensional change of the matrix and the microfibrils resulting from both the swelling and

114 restraint induced by NaOH treatment is examined to analyze anisotropic dimensional change.

115 Dimensional change in each direction is merely the sum of both contributions, assuming that the

116 matrix swelling is restricted by an unknown factor which is evaluated by swelling weight, that

117 each dimensional change is independent, and that change in the cell wall thickness is negligible

118 The above assumptions imply that each dimensional change is described by the geometrical sum

119 of the dimensional change of the microfibrils and that of the matrix with swelling weight.

120 Our model of anisotropic dimensional change also considers anisotropic microfibrils

121 embedded in an elastic isotropic matrix. Note that microfibrils are contractible and that the

122 microfibril angle is constant with NaOH treatment, as discussed below.

123 Nakano *et al.* (2000) derived the following equation for the longitudinal contraction of

124 wood treated with aqueous NaOH solution, assuming that distortion of the sample along the

125 longitudinal axis depended on both microfibril contraction and a change in the microfibril angle.

126
$$\frac{\Delta L}{L} = \frac{\Delta l}{l} + \frac{\Delta \cos\theta}{\cos\theta},$$

127 where L and l are the sample length along the longitudinal axis and the microfibril length,

128 respectively, $\cos\theta$ is the cosine of the microfibril angle θ, and $\Delta L/L$, $\Delta l/l$ and $\Delta\cos\theta/\cos\theta$

129 represent the relative change in each of these variables. This equation is essentially the same as

130 that of microfibrils derived by Sadoh and Kingston (1967) to discuss longitudinal shrinkage of

131 wood.   It should be noted that the longitudinal axis of microfibril differs from that of the sample.

132   Lindström *et al.* (1988) examined the dependence of swelling behavior on [NaOH] for

133 milled wood lignin (MWL), which is the main matrix of wood gelled by epichlorohydrin.   They

134 evaluated the swelling of MWL not by dimensional changes but by weight gain.   In their report,

135 the water gain (w/w) was maximal at 0.8 < [NaOH] < 1.6 meq/g.   The amount of weight gain

136 increased gradually with increasing [NaOH] and increased rapidly at [NaOH] > 20 meq/g.   This

137 demonstrated that at high NaOH levels, lignin swelling was dependant on NaOH concentration.

138   Considering dimensional change of the wood matrix with lignin, the above equation is

139 reduced to

$$\frac{\Delta L}{L} = \frac{\Delta l}{l} + \frac{\Delta \cos \theta}{\cos \theta} + K_1 \frac{\Delta m}{m} ,$$

141 where $\Delta m / m$ is the swelling ratio of the matrix and K_1 is the swelling weight of matrix along

142 the longitudinal axis of the sample. Restraint of matrix swelling is evaluated by the parameter

143 K_1, which is probably caused by microfibrils.   Figure 2 shows that the microfibril angle for Yezo

144 spruce was on average 8.7° and exhibited no dependence on [NaOH].   The result shown in

145 Figure 2 is different from the result by Fujimoto and Nakano (2000) that the fibril angle

146 depended on [NaOH] using the iodine method.   However, the results measured by X-ray

147 irradiation was adopted in this work.   This is because the X-ray diffraction method gives the

148 average value of the fibril angles, though the iodine method does the local information for some

149 cell walls.   For wood species with very small microfibril angles, such as those used in the current

150 study, where $\Delta \cos \theta = \Delta \theta \cdot \sin \theta \approx 0$, no dependence on [NaOH] was observed.   The above equation

151 then reduces to

$$\frac{\Delta L}{L} = \frac{\Delta l}{l} + K_1 \frac{\Delta m}{m} . \tag{1}$$

153   According to Equation (1), $K_1 \Delta m / m \approx 0$ was expected since the contribution of the wood

154 matrix to the change along the longitudinal direction was much smaller than that of microfibrils

155 because of the high elastic modulus of the microfibrils.   However, dimensional changes in wood

156 samples occur not only along the longitudinal axis but also along the radial and tangential axes

157 (Stöckmann, 1971a, 1971b; Ishikura and Nakano, 2007).   Due to the small microfibril angle,

158 changes along the latter axes need to be considered in terms of matrix contributions. That is
159 strikingly different from the dimensional change along the longitudinal axis. We will deal with
160 not the mechanical equilibrium between wood components but the dimensional change resulted
161 from both the swelling and restraint induced with NaOH treatment, as discussed below.

162   Expressions to describe the changes along the radial and tangential axes were initially
163 derived assuming that the wood cell wall consists of two phases: the cellulose microfibril and an
164 isotropic matrix, with a volume fraction microfibril / matrix = φ / $(1-\varphi)$, and microfibril angles of
165 the LT- and LR-planes in wood cell wall designated as θ_{LT} and θ_{LR}, respectively. Given this
166 model structure, shown schematically in Figure 3, with a small microfibril angle, the changes
167 along the radial and tangential axes of the sample are represented by

168
$$\frac{\Delta R}{R} = \phi \frac{\Delta l}{l} \sin \theta_{LR} + K_2 (1-\phi) \frac{\Delta m}{m} , \qquad (2)$$

169
$$\frac{\Delta T}{T} = \phi \frac{\Delta l}{l} \sin \theta_{LT} + K_3 (1-\phi) \frac{\Delta m}{m} , \qquad (3)$$

170 where the microfibril change along the longitudinal axis of itself is given by $\Delta l / l$, and
171 dimensional changes along the radial and tangential axes of the sample are given by $\Delta R / R$ and
172 $\Delta T / T$, respectively. Matrix contributions are represented by $\Delta m / m$. K_2 and K_3 are the
173 swelling weight and are related to the anisotropy restraint of the radial and tangential
174 orientations, respectively. or the Poisson ratio effect. If the Poisson ratio effect is different
175 between LT-plane and LR-plane of wood cell due to the longitudinal shrinking as well as that for
176 water sorption (Skaar, 1988), $\Delta T / T$ may be different from $\Delta R / R$. Considering that the
177 microfibril angle is sufficiently small and that $\Delta R / R < \Delta T / T$ over [NaOH] as shown in Fig.1, 0 <
178 $K_2 < K_3$ <1. Dimensional change perpendicular to the longitudinal axis of the microfibrils is
179 neglected in equations (2) and (3) because the contribution of $\Delta l / l$ is greater than that of the
180 change perpendicular to the longitudinal axis of microfibrils. The reason is that the Poisson's
181 ratio is   generally 0.3 or less for solid materials.

182

183

184 **Changes in sample cross section and microfibril contraction**

185

186   The following discussion will focus on the implications of these dimensional changes as

187   shown in Figure 1.   At [NaOH] > 0.10, the signs in Equations (2) and (3) follow from Figure 1:

188
$$\frac{\Delta R}{R} = \phi \frac{\Delta l}{l} \sin \theta_{LR} + K_2 (1-\phi) \frac{\Delta m}{m} < 0 ,$$
(4)

189
$$\frac{\Delta T}{T} = \phi \frac{\Delta l}{l} \sin \theta_{LT} + K_3 (1-\phi) \frac{\Delta m}{m} > 0 .$$
(5)

190   The sum of multiplying Equation (4) by K_3 and multiplying Equation (5) by $-K_2$ yields

191
$$\phi \frac{\Delta l}{l} (K_3 \sin \theta_{LR} - K_2 \sin \theta_{LT}) < 0 ,$$
(6)

192   Considering that $0 < \varphi < 1$, $0 < K_2 < K_3 < 1$ and $0 < \theta_{LT} < \theta_{LR} \ll 90°$ so that

193    $(K_3 \sin \theta_{LR} - K_2 \sin \theta_{LT}) > 0$ in Equation (6), the following expression is derived:

194
$$\frac{\Delta l}{l} < 0 .$$
(7)

195   The experimental results of $\Delta R / R < 0$ and $\Delta T / T > 0$ in Figure 1 require $\Delta l / l < 0$, that is, shows

196   that the microfibril contracts along its longitudinal axis with NaOH treatment when Equations

197   (1) to (3) are hold. The same result is also obtained from equation (1) because of

198    $\Delta l / l \approx \Delta L / L < 0$ due to $K_1 \Delta m / m \approx 0$.

199

Crystallinity changes and the location of the crystalline region

201

202   The above discussion suggests that microfibril contraction is the primary factor of

203   anisotropic changes in wood.   These changes can also be correlated with observed changes in the

204   crystallinity of the microfibril at NaOH concentrations greater than 0.10 (Fengel *et al.*, 1995).

205   Figure 4 shows the relationship between crystallinity and dimensional changes along the

206   longitudinal axis of samples.   Changes were calculated based on the corresponding wet

207   dimension at [NaOH] = 0.   Contraction of the wood sample increased with decreasing

208   crystallinity starting at [NaOH] = 0.10.   The change shown in Figure 4 implies that a decrease

209   in crystallinity causes contraction of the microfibril itself along the longitudinal axis, and hence

210   an overall contraction of the sample along the longitudinal axis.

211   Two hypotheses can be considered for the location of the amorphous region created in the

microfibril by NaOH treatment.　One hypothesis is that the amorphous region exists about the crystalline region as a square of side a few nm and expands with the cross section.　The other hypothesis is that the amorphous region forms at defects along the longitudinal axis of the microfibril which exist by about 20 nm and extends with a length along the longitudinal axis. The 20-nm length has been confirmed by leveling-off degree of polymerization (LODP) experiments and X-ray diffraction (Hayashi *et al.*, 1989).　The high linear correlation of $\Delta L / L$ as a function of crystallinity shown in Figure 4 suggests that NaOH treatment induces crystallinity changes in one of the aforementioned regions.　Nakano *et al.* (2000) reported that this change in crystallinity is localized in the longitudinal region of microfibril rather than the cross section.

Figure 5 shows the proposed combination mode of crystallinity of microfibers after NaOH treatment, where the crystallinity along the longitudinal and cross-sectional axes are w_c and h_c, respectively.　That is, they are the contribution of parallel and series to the longitudinal axis of microfibrils.　The gross crystallinity, ζ, is represented by

$$\zeta = h_c \cdot w_c, \tag{8}$$

This equation should not be a linear function of [NaOH] if the both crystallinity w_c and h_c have a [NaOH] dependence.　However, ζ as a function of NaOH concentration shows a highly correlated linear relationship, as shown in Figure 6. The crystallinity of wood samples ζ is approximately used as that of microfibrils in wood. This provides additional evidence that the crystallinity changes causes in either region of the both.　Therefore, it can be concluded that exposure to aqueous NaOH induces changes in crystallinity along the longitudinal axis, which in turn induces microfibril contraction.

he crystallinity of the wood samples were determined from X-ray diffraction data obtained on the LR-plane at 30 kV, 100 mA, and 2 °/min.　The degree of crystallinity was calculated from an the diffraction profile in the scanning range 10 – 32°.

242

Estimation of the microfibril angle

244

245   Substitution of Equation (1) into Equations (2) and (3) yields the following expressions

246   for $\Delta R / R$ versus $\Delta L / L$ and $\Delta T / T$ versus $\Delta L / L$, where $K_1 \Delta m / m$ is neglect because of

247    $K_1 \Delta m / m = 0.0010$:

248
$$\frac{\Delta R}{R} = \phi \frac{\Delta L}{L} \sin \theta_{LR} + K_2 (1-\phi) \frac{\Delta m}{m} , \qquad (9)$$

249
$$\frac{\Delta T}{T} = \phi \frac{\Delta L}{L} \sin \theta_{LT} + K_3 (1-\phi) \frac{\Delta m}{m} . \qquad (10)$$

250   Microfibril angles in the LR- and LT-planes can be calculated using the first derivatives of

251   Equations (9) and (10) as a function of $\Delta L / L$, which are confirmed by experimental results at

252   [NaOH] > 0.10 for $\Delta R / R$ versus $\Delta L / L$ and $\Delta T / T$ versus $\Delta L / L$. The second terms in both

253   equations are regarded as constant, since $\Delta R / R$ and $\Delta T / T$ are almost constant and $\Delta L / L = 0$

254   at [NaOH] < 0.10.

255   Experimental results yielded slope values of 0.0800 for $\Delta R / R$ versus $\Delta L / L$ and 0.0188

256   for $\Delta T / T$ versus $\Delta L / L$, with y-intercepts of 0.0045 and 0.0305, respectively. Accordingly,

257   microfibril angles of θ_{LR} = 9.20° and θ_{LT} = 2.15° were obtained. The former value agrees

258   reasonably well with the average microfibril angle observed in the LR-plane shown in Figure 2,

259   though the latter appears to be too little comparing the results reported (Nakato, 1958) In the

260   present report, these values were deemed valid and used in the below simulation.

261

Simulation of the anisotropic dimensional change

263

264   The main parameter affecting dimensional changes in the wood samples was

265   crystallinity changes as a result of the NaOH treatment shown in Figure 4. NaOH induces a

266   decrease in microfibril crystallinity, which causes contraction of the microfibril along the

267   longitudinal axis and ultimately a contraction of the wood sample along the longitudinal axis of

268   the sample. It should be noted that the longitudinal axis of microfibril differs from that of the

269   sample. Although this effect is manifest primarily along the longitudinal axis of the sample, the

270   tangential and radial regions are also considered in the below simulation.

271   From Equation (1), the dimensional change of the sample, $\Delta L / L$, with the

272   experimentally derived $K_1 \Delta m / m = 0.0010$, can be represented by

273
$$\frac{\Delta L}{L} = \frac{\Delta l}{l} + 0.0010 , \tag{11}$$

274   where the value 0.0010 represents the contribution of matrix swelling to the overall dimensional

275   change of the sample along the longitudinal axis at [NaOH] = 0.03 to 0.07 and is negligible small.

276   The value $\Delta L / L$ was calculated from the contraction of the microfibril, $\Delta l / l$, as shown in

277   Equation (11). Thus, determination of $\Delta L / L$ can be reduced to $\Delta l / l$, which in turn can be

278   evaluated from the end-to-end distance of the amorphous cellulose chain along the longitudinal

279   axis of the microfibril.

280   It is difficult to know the actual behavior of the cellulose chain when both ends may be

281   bound to a crystalline region, though some researchers reported the simulation of conformation of

282   single cellulose chain in this regard (for example Queyroy et al., 2004). Additionally, the

283   end-to-end distance of the cellulose chain appears to be slightly influenced by non-crystallization

284   because of a non-flexible polymer chain. Therefore, the classical method by Benoit (1947), using

285   the characteristic parameter α to represent a corrected deviation from the free jointed chain

286   model, was utilized herein.

287   As well-known, the end-to-end distance of the cellulose chain is represented by $0.79\sqrt{N}$

288   for the unit number N when the appropriate constants are substituted in Benoit's equation: a C –

289   O bond length of 0.143 nm, a length between C_1 and C_4 equal to 0.298 nm, and angles COC and

290     $C_1 C_4 O$ of 110° and 150°, respectively. Benoit's equation requires the correction term α,

291   representing the length of the free jointed chain model. For example, α is typically 2–5 for

292   cellulose tributylate and cellulose tricaplate and about 2 for polyethylene. The former values

293   are representative of a rod-like polymer conformation and the latter has a simple, flexible

294   structure. Thus, the length of the amorphous region along the longitudinal axis of microfibril

295   l_a is described by $l_a = 0.79\alpha\sqrt{N}$.

296   The change in microfibril length, $\Delta l / l$, can be represented by the degrees of

297   non-crystallization of microfibrils with NaOH treatment, with microfibril length, the length of a

298   glucose residue, and crystallinity along the longitudinal axis given by l_u , l_g , and $h_c (= \zeta / w_c)$,

299   respectively:

$$\frac{\Delta l}{l} = \left(l_u \cdot h_c + 0.79\alpha\sqrt{\frac{l_u(1-h_c)}{l_g}} \right) / l_u - 1 \tag{12}$$

301 The first and second terms in parentheses of Equation (12) are the length of the crystalline and

302 amorphous regions, respectively. The first term in Equation (12) is the ratio of microfibril

303 length after / before NaOH treatment. The microfibril length l_u is the period determined from

304 LODP and X-ray diffraction with 20nm. Substituting $l_u = 20$ nm and $l_g = 0.515$ nm into

305 Equation (12) and then substituting this result into Equation (11) yields

$$\frac{\Delta L}{L} = \left[\left(20 \cdot h_c + 0.79\alpha\sqrt{\frac{l_u(1-h_c)}{0.515}} \right) / 20 - 1 \right] \cos\theta + 0.0010 \tag{13}$$

307   Dimensional changes in the wood samples as a function of crystallinity induced by

308 NaOH treatment can now be simulated using Equations (8) and (13). The simulation variables

309 were $h_c (= \zeta / w_c)$ and α, since the empirical microfibril angles were small (θ_{LR} = 9.20° and θ_{LT} =

310 2.15° so that $\cos\theta_{LR} \approx \cos\theta_{LR} \approx 1$). Typical results in Figure 7 show that the most accurate

311 simulations were obtained with α = 3, when $w_c = 1.00$ and then $h_c (= \zeta / w_c) = 0.522$ where $\underline{\zeta}$ the

312 gross crystallinity. This implies that changes in crystallinity occurred only along the

313 longitudinal axis of microfibrils and that that the amorphous cellulose chains are extended.

314   Table 1 shows the results obtained with α = 2.5 and 3. The degree of contraction

315 calculated from the ratio of end-to-end distance to contour length was about 0.10–0.20.

316 According to analyses of single cellulose chains by Queyroy *et al.* (2007), the end-to-end distance

317 of a chain consisting of eight glucose residues with a contour length of 4.4 nm is about 3.2 nm.

318 This corresponds to a 0.30 contraction. Considering N = 13 to 26 in this work and N = 8 in

319 Queyroy's simulation, the former is much smaller than the latter. This may simply result from

320 the different calculation methods employed. However, the most likely reason is that both ends

321 of the amorphous cellulose chains bond to the crystalline regions and are therefore unable to

322 satisfactorily contract. This conclusion is also supported by the simulation results obtained with

323 α = 3.

324   The observed changes in the radial and tangential directions, $\Delta R / R$ and $\Delta T / T$, were

325 also simulated based on derivations from Equations (9) and (10). Simulation requires the

326 parameters K_1 and K_2. Their contribution can be estmated using $\Delta R / R$ and $\Delta T / T$ at [NaOH]

327 < 0.10 since the microfibril does not contract at [NaOH] < 0.10, where dimensional changes are

328 due to changes in the matrix only:

329
$$\frac{\Delta R}{R} = K_2(1-\phi)\frac{\Delta m}{m} \tag{14}$$

330
$$\frac{\Delta T}{T} = K_3(1-\phi)\frac{\Delta m}{m} \tag{15}$$

331 Both $\Delta T/T$ and $\Delta R/R$ varied little at [NaOH] < 0.1 and were regarded as constant Empirical

332 results were $\Delta R/R = K_2(1-\phi)\Delta m/m = -0.0037$ and $\Delta T/T = K_3(1-\phi)\Delta m/m = 0.0217$. Similarly,

333 $K_1\Delta m/m = 0.0010$ was obtained from empirical result at [NaOH] < 0.1 and Equations (1). That

334 is, K_1 and K_2 are almost 0 and $K_3 > 0$ at [NaOH] < 0.1, considering swelling of matrix. This fact

335 suggests strong restraint along the longitudinal and radial axes and little restraint along

336 tangential axis.

337 As shown in Fig.1, $\Delta T/T$ was constant swelling and $\Delta R/R$ varied little at [NaOH]

338 between 0.03 and 0.10 where no longitudinal shrinking. This fact suggests that wood matrix is

339 only slightly dependent on NaOH concentration though it swells due to the NaOH treatment.

340 Thus, assuming that dimensional changes in the wood matrix were constant over [NaOH] = 0.03

341 to 0.20, $\Delta T/T$ and $\Delta R/R$ were calculated using Equations (2) and (3). The most accurate results

342 for $\Delta L/L$ were obtained with α = 3, $h_c = 0.522$, $w_c = 1.00$, θ_{LT} = 2.15°, and θ_{LR} = 9.20°. These

343 results are shown in Figure 1 as solids lines which are best fitting and show good agreement

344 between experimental and calculation data. Some disagreement, however, can be observed

345 along the tangential axis and may be due to the Poisson ratio effect, which was not accounted for

346 in these simulations. Low microfibril angles allow the matrix to swell easily along the in

347 tangential axis. Additional changes due to the Poisson effect may then be caused by shrinking

348 along the radial axes. This effect may also contribute to the observed discrepancy between

349 experimental and theoretical results in Figure 1 at [NaOH] > 0.10.

350

351 **Conclusion**

352

353 Anisotropic swelling of wood samples with treatment with aqueous NaOH solution at 0

354 to 0.20 fraction concentrations was examined. At NaOH concentrations less than 0.10, swelling

355 occurred only along the tangential axis (T) and not along the radial (R) or longitudinal (L) axes.

356 At greater NaOH levels, the swelling was even more pronounced along T, with shrinkage along

357 the other axes.   These anisotropic changes along R and L were closely related to the longitudinal

358 crystallinity change of microfibrils in the wood cell wall and were simulated with the cell

359 structure model.   This exercise revealed microfibril contraction and matrix swelling in the wood

360 cell wall upon NaOH treatment. That is, the characteristic dimensional changes in wood with

361 NaOH treatment are due to the decreasing crystallinity of microfibrils, matrix swelling, and

362 differences in microfibril angles in the LP- and LT- planes of the wood cell wall. The main factor

363 is microfibril contraction along the longitudinal axis with decreasing crystallinity in the

364 microfibrils. The results obtained in this analysis illustrate the complex interaction between

365 microfibrils and the matrix and may serve as a new basis for understanding the anisotropic

366 swelling and shrinkage of wood.

367

368

369 **Acknowledgements**

370

374 **References**

375 Barber NF, Meylan BA (1964) The anisotropic shrinkage of wood. Holzforschung 18: 146-156

376 Benoit H (1947) Sur la statique des chains avec interactions et empechements ateriques. J Chem

377　　 Phys 44: 18–21

378 Fengel D, Jakob H, Strobel C (1995) Influence of the alkali concentration on the formation of

379　　 cellulose II. Holzforschung 49: 505–511

380 Fratzl P, Elbaum R, Burgert I (2008) Cellulose fibrils direct plant organ movement. Faraday

381　　 Discussion 139: 275-282

382 Hayashi J, Ishizu A., Isogai A (1989) Chemistry and solid state structure of cellulose. Sen-i

383　　 Gakkaishi 45: 469-480

384 Ishikura Y., Nakano T (2007) Contraction of the microfibrils of wood treated with aqueous NaOH.

385　　 J Wood Sci 53: 175–177

386 Lindström T, Wallis A, Tulonen J, Kolseth P (1988) The effect of chemical environment on

387　　 swelling and dynamic mechanical properties of milled wood lignin gels. Holzforschung 42:

388　　 225–228

389 Nakato K. (1958) On the cause of the anisotropic shrinkage and swelling of wood IX (in Japanese).

390　　 Mokuzai Gakkaishi 4: 134–141

391 Nakano T (1988a) Plasticization of wood by alkali treatment (in Japanese). Nihon Reoroji

392　　 Gakkaishi (Journal of the society of Rheology, Japan) 16(1): 48–49

393 Nakano T (1988b) Plasticization of wood by alkali treatment effects of kind of alkali and

394　　 concentration of alkaline aqueous solution on stress relaxation (in Japanese). Nihon Reoroji

395　　 Gakkaishi (Journal of the society of Rheology, Japan) 16(3): 104–110

396 Nakano T (1989) Plasticization of wood by alkali treatment.　 Relationship between

397　　 plasticization and the ultra-structure (in Japanese). Mokuzai Gakkaishi 35(5): 431–437

398 Nakano T, Sugiyama J, Norimoto M (2000) Contraction force and transformation of microfibril

399　　 with aqueous sodium hydroxide solution. Holzforschung 54: 315–320

400 Preston, R.D.　 1942. Anisotropic contraction of wood and its constituent cells. Forestry, 16,

401　　 32-48.

402 Queyroy S, Müller-Plathe F, Brown D (2004) Molecular dynamics simulations of cellulose

403　　 oligomers conformational analysis. Macromol Theory Simul 13: 427–440

404 Sadoh T, Kingston RST (1967) Te relation between longitudinal shrinkage and structure. Wood &

405   Technol. 1: 81-98

406 Salmén L, Burgert I (2009) Cellwall features with regard to mechanical performance.

407   Holzforschung 63: 121-129

408 Skaar, C. (1988) Wood-Water Relations. Springer, Berlin Heidelberg New York London Paris

409   Tokyo, pp 155-156

410 Stöckmann VE (1971a) Effect of pulping on cellulose structure Part I. Tappi 54(12): 2033–2037

411 Stöckmann VE (1971b) Effect of pulping on cellulose structure Part II. Tappi 54(12): 2038–2045

412 Fujimoto T, Nakano T (2000) The effect of mercerization on wood structural features. Mokuzai

413   Gakkaishi 46(3): 238-241

414 Yamamoto H, Kojima Y, Okuyama T, Abasolo WP (2002) Origin of the biomechanical properties of

415   wood related to the fine structure of the multi-layered cell wall. J Biomechanical Eng 124:

416   432-440

Figure captions
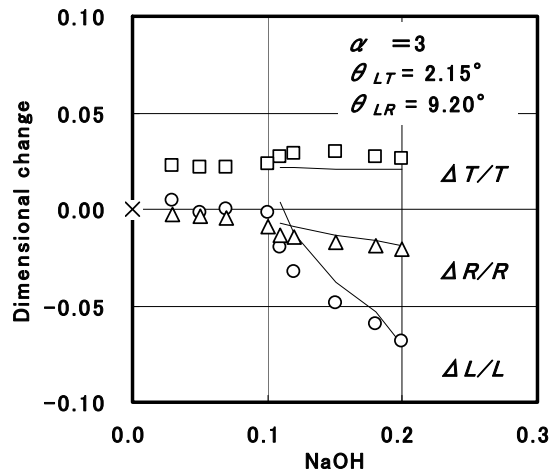
Fig. 1. Experimental (plots) and best fitting (solid lines) results of dimensional changes along the radial ( ), tangential (□), and longitudinal (○) axes as functions of the NaOH aqueous solution. Note: α = 3, $\theta_{LT} = 2.15°$ and $\theta_{LR} = 9.20°$.

Fig. 2. Dependence of microfibril angle on the concentration of aqueous NaOH solution.

Fig. 3. The cell wall model for anisotropic dimensional changes consisted of matrix and microfibril components. Note: θ = fibril angle, φ = volume fraction of the microfibril.

Fig. 4. Dimensional changes along the longitudinal axis of treated wood as functions of crystallinity.

Fig. 5. A schematic diagram for the crystalline and amorphous regions of a microfibril.
Note: w_c and h_c are crystallinity of micro fibril in cross section and longitudinal directions.

Fig. 6. Relationship between crystallinity and concentration of aqueous NaOH solution for Yezo spruce treated with aqueous NaOH solution.

Fig. 7. Typical experimental (open circle) and simulated (solid line) results of dimensional changes along the longitudinal axis of wood samples. Note: θ = fibril angle; α = characteristic ratio; w_c = crystallinity of the cross section.

Table 1. Typical end-to-end distances, representing the highest degree of agreement between experimental and theoretical results in amorphous regions of 20-nm microfibrils.

Note: w_c = crystallinity of the cross-sectional area; h_c = crystallinity of the longitudinal area; N = number of glucose residues in the amorphous region; α = characteristic ratio.

| Crystallinity ζ | w_c = 1.00 | | | w_c = 0.70 | | |
| | | | α =3 | | | α =2.5 |
	h_c	N	Distance (nm)	h_c	N	Distance (nm)
0.459	0.459	21	10.9	0.656	13	7.2
0.428	0.428	22	11.2	0.611	15	7.7
0.380	0.380	24	11.6	0.543	18	8.3
0.351	0.351	25	11.9	0.501	19	8.7
0.320	0.320	26	12.2	0.457	21	9.1

Fig. 1. Experimental (plots) and best fitting (solid lines) results of dimensional changes along the radial ( ), tangential (□), and longitudinal (○) axes as functions of the NaOH aqueous solution.   Note: α (characteristic ratio of polymer conformation)= 3, $\theta_{LT} = 2.15°$ and $\theta_{LR} = 9.20°$.
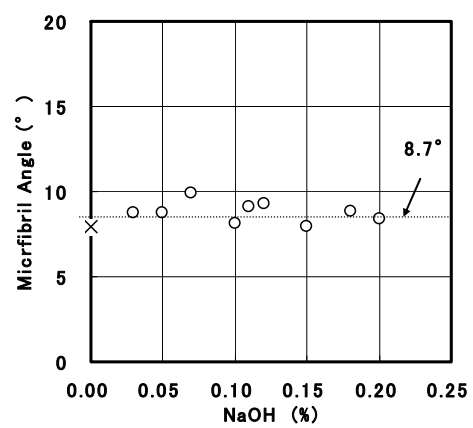
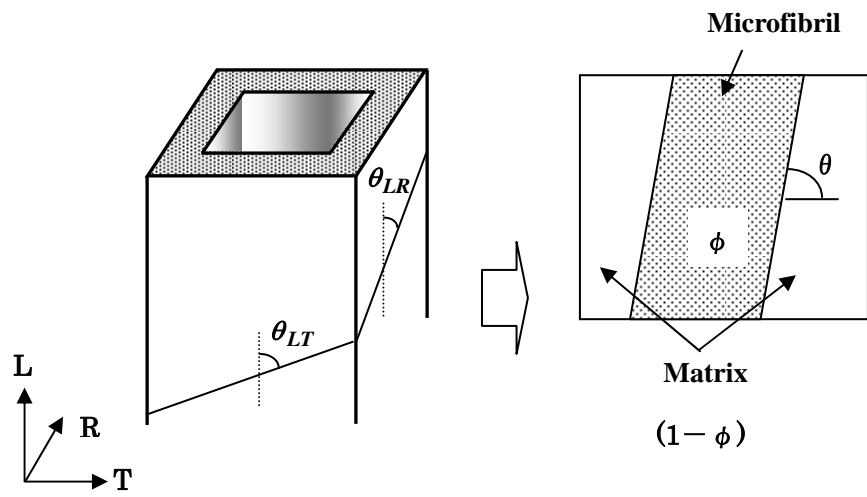Fig. 2.   Dependence of microfibril angle on the concentration of aqueous NaOH solution.

Fig. 3.   The cell wall model for anisotropic dimensional changes consisted of matrix and microfibril components.   Note: θ = fibril angle, φ = volume fraction of the microfibril.
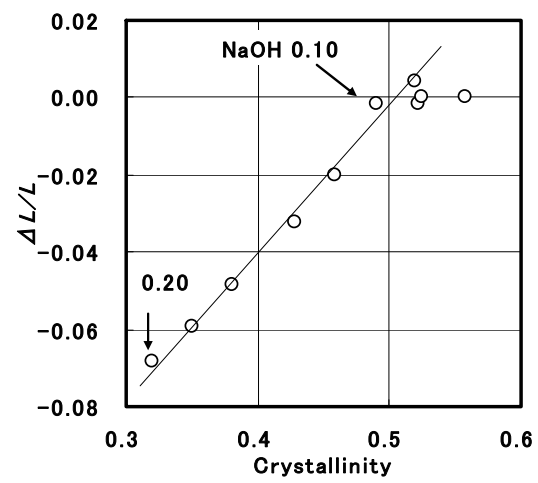
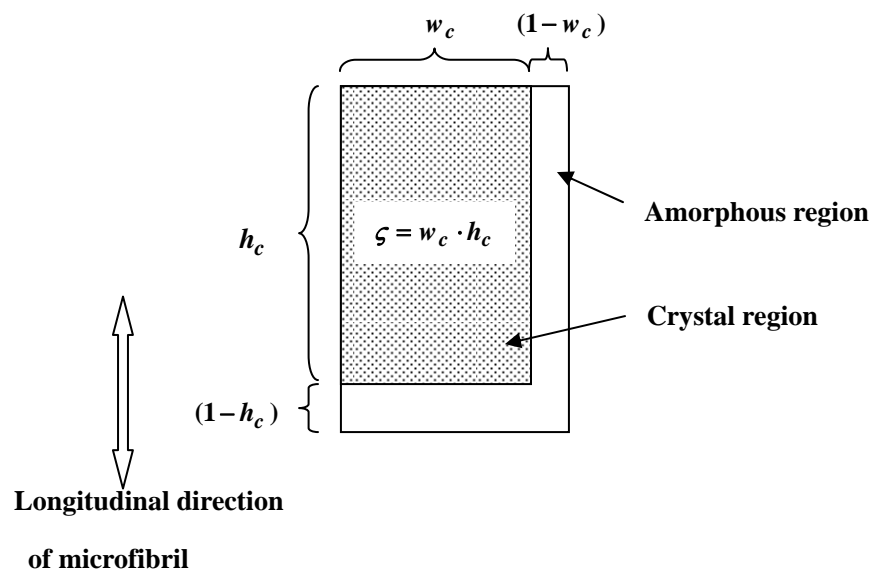Fig. 4. Dimensional changes along the longitudinal axis of treated wood as functions of crystallinity.

Fig. 5. A schematic diagram of combination mode for the crystalline and amorphous regions of a microfibril. Note: w_c and h_c are crystallinity of micro fibril in cross section and longitudinal directions.
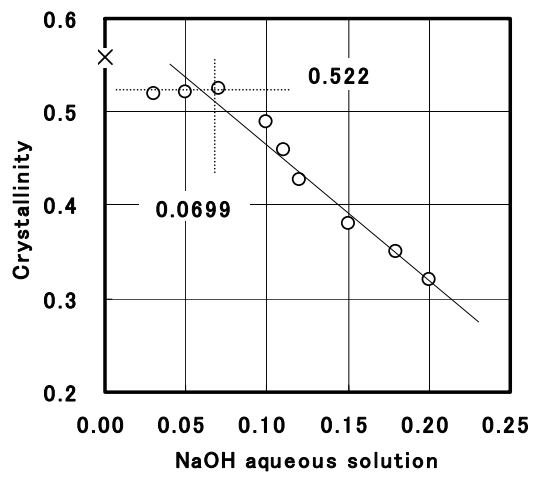
Fig. 6.　Relationship between crystallinity and concentration of aqueous NaOH solution for Yezo spruce treated with aqueous NaOH solution.
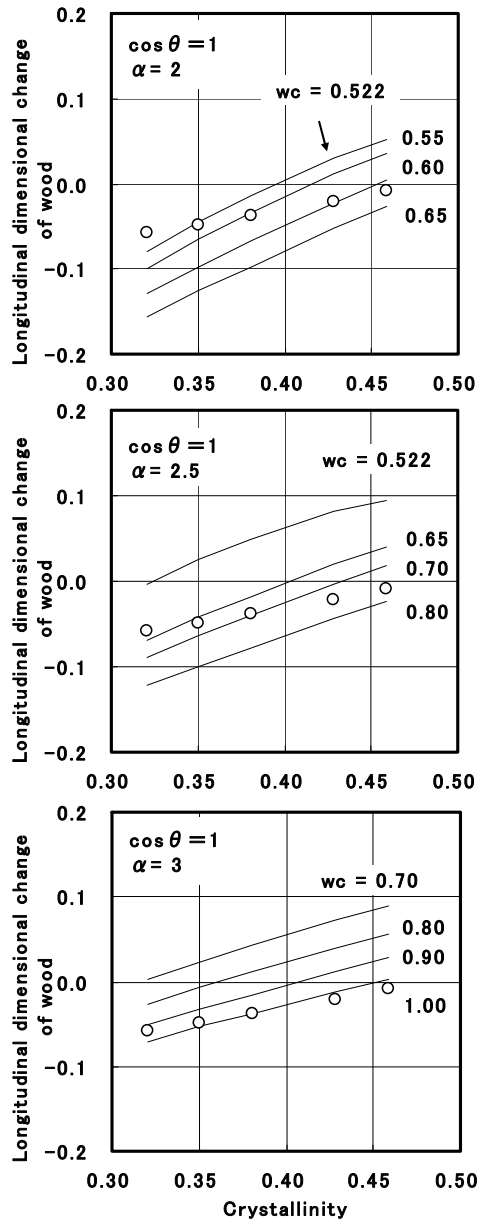
Fig. 7. Typical experimental (open circle) and simulated (solid line) results of dimensional changes along the longitudinal axis of wood samples. Note: θ = fibril angle; α = characteristic ratio; w_c = crystallinity of the cross section.